THE JOURNAL OF PHYSICAL CHEMISTRY Letters

Letter

Cite This: J. Phys. Chem. Lett. 2018, 9, 2909−2913

pubs.acs.org/JPCL

Simple-to-Complex Transformation in Liquid Rubidium

Federico A. Gorelli,[†,‡] Simone De Panfilis,*[,§] Taras Bryk,[∥] Lorenzo Ulivi,[⊥] Gaston Garbarino,[#] Paraskevas Parisiades,[#] and Mario Santoro[†,‡]

[†]INO-CNR, I-50019 Sesto Fiorentino, Italy

[‡]LENS, European Laboratory for Non Linear Spectroscopy, I-50019 Sesto Fiorentino, Italy

[§]Center for Life Nano Science IIT@Sapienza, Istituto Italiano di Tecnologia, I-00161 Roma, Italy

[∥]Institute for Condensed Matter Physics of NASU, UA-79011 Lviv, Ukraine

[⊥]IFAC-CNR, I-50019 Sesto Fiorentino, Italy

[#]European Synchrotron Research Facility, FR-38043 Grenoble, France

ABSTRACT: We investigated the atomic structure of liquid Rb along an isothermal path at 573 K, up to 23 GPa, by X-ray diffraction measurements. By raising the pressure, we observed a liquid−liquid transformation from a simple metallic liquid to a complex one. The transition occurs at 7.5 ± 1 GPa which is slightly above the first maximum of the T−P melting line. This transformation is traced back to the density-induced hybridization of highest electronic orbitals leading to the accumulation of valence electrons between Rb atoms and to the formation of interstitial atomic shells, a behavior that Rb shares with Cs and is likely to be common to all alkali metals.

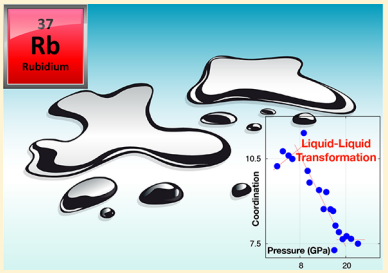

In the last 20 years an increasingly growing number of discoveries of liquid polymorphism appeared in the literature.[1−4] Liquid−liquid transformations (LLTs) have been suggested by simulations to occur in correlation with changes of the directional bonding in molecular liquids such as water[5−8] and fused quartz[9] or else in atomic liquids such as Si.[10−13] On the other hand, LLTs have been experimentally discovered in some elemental liquids[14−24] and more complex systems.[25]

The thermodynamics of these transitions was addressed by Rapoport,[26] who related the presence of melting-curve maxima in the phase diagram of pure substances, as in Rb and Cs, to the existence of more than one liquid structure at constant chemical composition. At a microscopic level, the transformations between liquid phases are likely to be correlated to metallization or polymerization processes and, in general, to changes of the electronic structure which in turn lead to modifications of the atomic interactions and/or bonding.

In the specific case of Cs, relevant electronic changes in this respect involve *s*−*p*−*d* or *s*−*d* hybridization.[19,27] In Rb this phenomenon is expected to lead to a spatial localization of valence electrons and, as a consequence, to an increased directional character of interatomic interactions toward the potential formation of chemical bonds: The structure of liquid Rb is predicted to change from a simple liquid at low pressures to a complex one at high pressures.[28] Analogous electronic changes also largely affect alkali metal structure in the solid state, as the metal-to-insulator (semiconductor) phase transition experimentally observed in the Mbar pressure range.[29,30]

Similarly to all known alkali metals, Rb has a complex phase diagram (see Figure 1) showing a sequence of six crystalline phases by increasing pressure. It adopts close-packed crystal structures at both high and low pressures, while it exhibits low coordination and conductivity and higher crystal complexity at intermediate pressures.[31] The melting curve has been

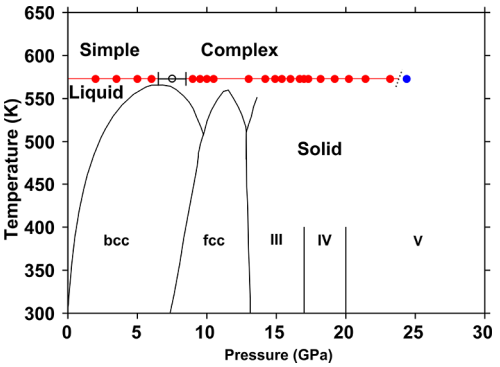

Figure 1. Known phase diagram of Rb below 30 GPa. Six different structural phases of solid Rb have been experimentally observed below 100 GPa,[34,35] including the modulated Rb−III[36] and the incommensurate Rb−IV[37,38] comprised of a tetragonal host framework and a simple body-centered tetragonal guest. The red line represents the isotherm followed in the present experiment. The red dots represent the experimental points in the liquid phase. The blue dot represents the point where the sample has crystallized upon compression. The empty symbol marks the anomaly in the liquid structure evolution discovered in this work. The black dashed line represents the expected melting line.

Received: April 9, 2018
Accepted: May 15, 2018
Published: May 15, 2018

DOI: 10.1021/acs.jpclett.8b01094
J. Phys. Chem. Lett. 2018, 9, 2909−2913

experimentally reported only up to 14 GPa,[32] while the structure of liquid Rb has never been experimentally investigated at pressures higher than 6.1 GPa.[33] Recently, we performed an ab initio molecular dynamics (AIMD) study of liquid Rb along an isotherm at 573 K, shedding new light onto the structural and dynamic features under high pressure.[28] These AIMD calculations extended up to about 30 GPa, unveiling a breakdown of the nearly free-electron model occurring in the liquid state at 12.5 GPa. Here we report on an X-ray diffraction (XRD) experimental study of liquid Rb along an isothermal compression at 573 K up to the melting line, aimed at experimentally verifying the presence of the predicted structural transformation between simple and complex liquids.

XRD patterns were collected along an isotherm at 573 K, up to the crystallization occurring at about 24 GPa, and selected $S(Q)$ from two different samples in two independent pressure runs are shown in Figure 2 as a function of pressure. By

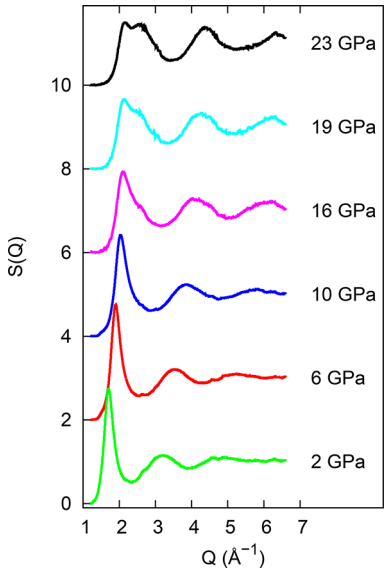

Figure 2. Pressure evolution of the static structure factor $S(Q)$ of liquid Rb along the isotherm at 573 K as obtained by XRD experiments. A constant vertical shift of 2 between adjacent pressure $S(Q)$ curves was applied for practical graphical reasons. The patterns have been measured in two independent runs, on two different samples, with good reproducibility.

increasing pressure, we observe the appearance of a shoulder at high Q of the main diffraction peak of the $S(Q)$. This feature evolves up to a double peak at the maximum pressure of the experiment, showing two components of similar intensity. This dramatic change is reproducible along compression and decompression cycles and is qualitatively analogous, but with the opposite pressure trend, to that occurring in liquid water which, on the contrary, tends to become a simple molecular liquid at extreme conditions.[39] By reversing the argument, liquid Rb shows a transition from a simple metallic liquid at low pressures to a complex one at high densities. This qualitative argument is in agreement with our previous AIMD calculations,[28] which showed the accumulation of valence electronic charges in the interstitial volume between Rb atoms by increasing the pressure, suggesting the formation of quasi-covalent bonds.

To interpret these changes it is useful to examine the pair correlation function $g(R)$ in real space R. We obtain the $g(R)$ from the experimental $S(Q)$ following the iterative procedure described by Eggert et al.,[40] which also allows us to estimate the density values as a side product of the protocol. To suppress the termination ripples in the Fourier transform of experimental $S(Q)$s we used the revised Lorch modification function proposed in a recent article,[41,42] allowing the broadening Δ of the modifying function to increase with R. We used the AIMD determined densities,[28] interpolated at the experimental pressure points, as initial seed for the iterative data reduction. Our experimental estimation of the density results to be in excellent agreement with the simulated one as shown in Figure 3.

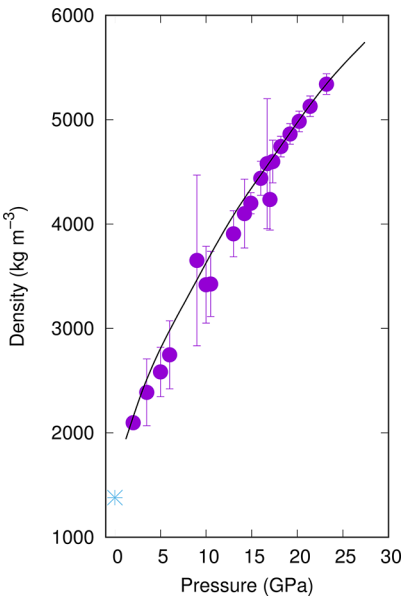

Figure 3. Equation of state of liquid Rb at 573 K as calculated by the iterative procedure discussed in the text. Purple symbols: this work. Continuous line: AIMD density from ref 28. Blue cross: density at ambient pressure and 573 K from ref 43.

In Figure 4 we show the pair correlation function $g(R)$ obtained from the experimental data following this method at several pressures and the corresponding quantities calculated with our previous AIMD simulation study at close pressures. The qualitative behavior of the two sets of data is in excellent agreement: as the pressure rises, new peaks appear between the first and the second coordination shells, at about 4.8 Å, and between the second and the third coordination shells, at about 7.3 Å, consistent with a complex local atomic arrangement scenario as previously discussed.[28] Of course, the quantitative comparison between the two sets of data, experimental and computational, is mainly hampered by the known over-structuring effect[44,45] rising at high pressure as a consequence of specific exchange-correlation functional (the generalized gradient approximation in Perdew–Burke–Ernzerhof form) used in the AIMD simulations.

Given the pair correlation function, a useful parameter to definitively solve the structure of a liquid substance and to address the occurrence of some transformation in the local environment is the nearest-neighbor coordination number. We estimated this quantity by fitting the $g(R)$ with gaussians and evaluating the integral of the Gaussian used for the first peak. In the bottom panel of Figure 5, we show the pressure evolution of the coordination number obtained in this way from both the

DOI: 10.1021/acs.jpclett.8b01094
J. Phys. Chem. Lett. 2018, 9, 2909–2913

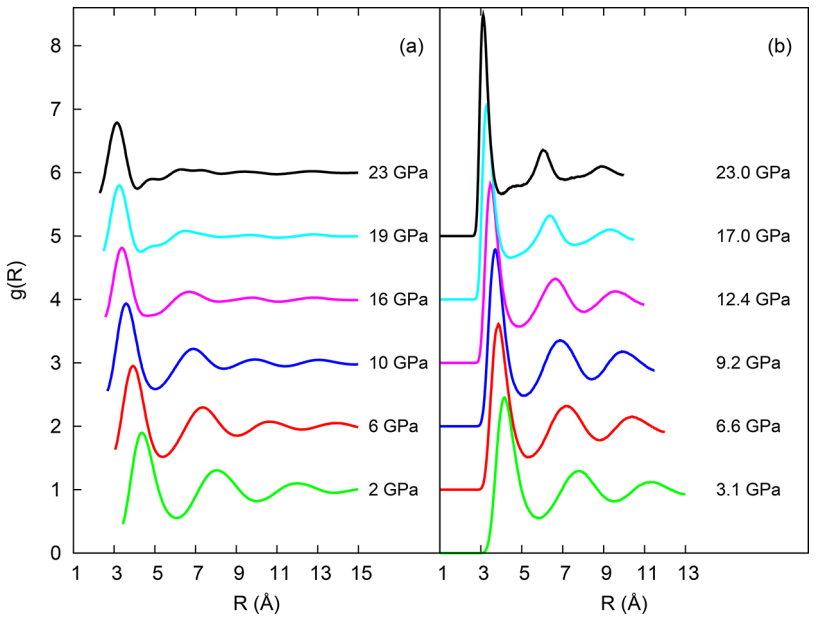

Figure 4. Pressure evolution of the pair correlation function $g(R)$ of liquid Rb along the isotherm at 573 K. (a) Results obtained by Fourier transform of the experimental static structure factor. (b) AIMD simulated pair correlation functions.[28]

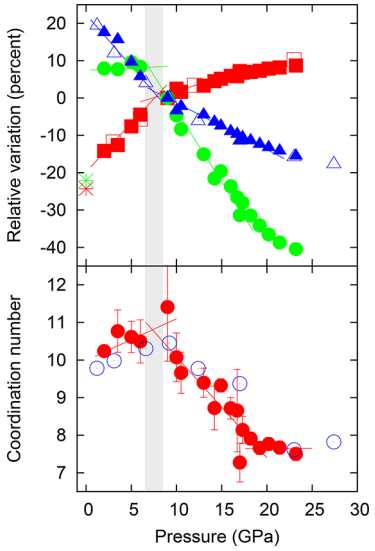

Figure 5. Top panel: pressure evolution at 573 K of the intensity (green dots) and position (red squares) of the main peak of the $S(Q)$ and of the position of the first peak of the $g(R)$ (blue triangles). Open symbols: AIMD values for the first peak of the $S(Q)$ and of the $g(R)$. Asterisks: ambient pressure values.[46] Bottom panel: coordination number as obtained from the experiment (full red dots) and AIMD simulations from ref 28 and adding 0.8 atoms for better comparison (empty blue dots). Continuous lines serve as guides to the eye and cross at the pressure where the simple-to-complex transformation takes place (shaded area).

experimental and simulated $g(R)$. For better comparison between the two sets of data, we added a rigid shift of 0.8 atoms to the simulated $g(R)$ to compensate for the over-structuring.

The top panel of Figure 5 shows the evolution of the intensity of the main peak of the $S(Q)$ with pressure manifesting an abrupt change of slope between 6.5 and 8.5 GPa. The pressure region where this anomalous behavior occurs, marked as a shaded area, is relatively small. It is beyond the interpretation of the present data to establish the type of transition. The steep decrease of the intensity of the main peak above 7.5 GPa, confirms the departure from the simple liquid model and the presence of a new compression mechanism of liquid Rubidium at high pressures. Consistently also the position of the main peak of the $S(Q)$ shows two quasi linear dependencies with pressure again crossing at about the same pressure. The quite evident slope change of these observables allows us to locate specific pressure at 7.5 ± 1 GPa between a simple hard-sphere-like liquid and a complex one. Experimental and simulation evolutions with pressure of the position of the first peak of the $g(R)$ also nicely agree, even if this trend does not seem to provide the same sudden change as the $S(Q)$ details. Very importantly, at above this pressure point we observe a continuous decrease of the coordination number evolving from about 11, which is close to 12, the limit value for a hard sphere system, to less than 8 above 20 GPa, where it remains almost constant up to the highest pressure of the experiment. This observation indicates that the densification of liquid Rb takes place along the counterintuitive reduction of the number of nearest neighbors, which is balanced by the formation of new interstitial shells, in agreement with our previous AIMD calculations[28] and with the works on Cs.[19,27] This transformation can so be traced back to the density-induced hybridization of highest electronic orbitals leading to the accumulation of valence electrons between Rb atoms and to the formation of interstitial atomic shells, a behavior that Rb shares with Cs and is likely to be common to all alkali metals. It is worthy to remark that the transformation pressure between simple and complex liquids is very close to the pressure of the first maximum of the melting line. Expanding the analogies with the water case[6,39] as discussed above, we may infer that the anomalous behavior observed in liquid Rb around 7.5 GPa mirrors the existence of a liquid−liquid phase transition line terminating in a critical point embedded in the undercooled liquid, compatible with the two-liquid model proposed by Rapoport[26] to explain liquidus maxima in pure substances. It is worthy to mention, though, that our previous AIMD

DOI: 10.1021/acs.jpclett.8b01094
J. Phys. Chem. Lett. 2018, 9, 2909−2913

simulations[28] indicate a slight volume jump, i.e., a first-order phase transition, at about 12 GPa, compatible with the transformation we experimentally observe.

In conclusion we have investigated the structural properties of liquid Rb in the pressure range extending between 2 and 23 GPa along an isotherm at 573 K, and we have observed a simple-to-complex liquid transformation at 7.5 ± 1 GPa. While at low pressure liquid Rb behaves as a quasi-hard-sphere system, in agreement with previous literature, and by increasing the pressure it acts as if bonds form up, showing significant extra atomic density between the first and second main shells and also between the second and third ones. The scenario is in overall agreement with our previous simulation study. This work provides further evidence of a nonisomorphic behavior in liquid alkali metals, as it occurs in liquid Cs and opens the way to a generalization of this phenomenon to all liquid alkali metals which will stimulate future investigations.

High purity Rb (99%) has been loaded in membrane-driven diamond anvil cells (DACs) equipped with 300 μm culet diamonds and a Re gasket. Maximum care has been taken to avoid contamination during the entire experimental protocol. DACs were loaded inside a glovebox under a dry and oxygen-free atmosphere (<0.5 ppm of O_2 and <0.5 ppm of H_2O) to prevent sample oxidation. To further avoid any chemical reaction, no pressure-transmitting medium was used. Pressure was determined by measuring the diffraction pattern from the edge of the Re gasket, which is in contact with Rb, and employing the known high-temperature Re equation of state.[47] XRD patterns of the low-pressure bcc and fcc phases recorded before the melting showed no trace of contaminant peaks, confirming the sample purity.

In order to heat the sample to the desired temperature, we used an external resistive coil heater designed for operation inside a vacuum chamber (Tempco Ltd.), which allows for stable heating of the whole DAC up to 1000 K. A K-type thermocouple, placed close to the diamond anvil, was used to measure the temperature of the sample. The uncertainty in sample temperature was estimated to be less than 10 K. At each pressure, the temperature was stable within 1 K during the X-ray exposure. The DAC was resistively heated inside a vacuum chamber equipped with Kapton windows and placed on a 6-axes sample stage at the ID27 beamline of the European Synchrotron Radiation Facility (ESRF).[48] A 33 keV monochromatic beam (0.3738 Å) focused down to the 3 × 2 μm^2 (H × V) spot, to avoid any scattering from the gasket, and MAR345 detectors were used to measure the angle-dispersive diffracted intensity. XRD patterns of solid and liquid Rb were collected in transmission geometry, over a diffraction cone equivalent to a maximum exchanged momentum Q_{max} of about 8 $Å^{-1}$. The sample−detector distance and the detector tilt angles were calibrated using powder diffraction from a CeO_2 standard at ambient conditions. Geometric and polarization corrections were taken into account during the angular integration.

Intensity integration and angular transformation to the exchanged momentum Q were completed via the Dioptas software.[49] Empty-cell background XRD patterns were obtained from the crystalline sample at high pressure, at the same temperature of the isotherm. The integrated scattering pattern of the empty cell is dominated by the Compton scattering of diamonds and air and was subtracted from the raw integrated pattern of the sample. Angular-dependent sample transmission and polarization corrections were used to compute 1-D raw sample intensities. The integrated 1-D intensity data were then reduced to obtain the total scattering function $S(Q)$ following an established protocol.[40]

AUTHOR INFORMATION

Corresponding Author

*E-mail: simone.depanfilis@iit.it.

ORCID

Simone De Panfilis: 0000-0002-9428-079X
Lorenzo Ulivi: 0000-0002-3541-0419
Mario Santoro: 0000-0001-5693-4636

Notes

The authors declare no competing financial interest.

ACKNOWLEDGMENTS

F.A.G., M.S., and L.U. acknowledge the PRIN project ZAPPING, number 2015HK93L7, granted by the Italian Ministry of Education, Universities and Research, MIUR, supporting their research in high-pressure materials science.

REFERENCES

(1) Wilding, M. C.; Wilson, M.; McMillan, P. F. Structural Studies and Polymorphism in Amorphous Solids and Liquids at High Pressure. *Chem. Soc. Rev.* **2006**, *35*, 964−986.

(2) Machon, D.; Meersman, F.; Wilding, M. C.; Wilson, M.; McMillan, P. F. Pressure-Induced Amorphization and Polyamorphism: Inorganic and Biochemical Systems. *Prog. Mater. Sci.* **2014**, *61*, 216−282.

(3) McMillan, P. F. Polyamorphic Transformations in Liquids and Glasses. *J. Mater. Chem.* **2004**, *14*, 1506−1512.

(4) Giovambattista, N. *Liquid Polymorphism*; Wiley-Blackwell, 2013; pp 113−138.

(5) Tanaka, H. A Self-Consistent Phase Diagram for Supercooled Water. *Nature* **1996**, *380*, 328.

(6) Poole, P. H.; Sciortino, F.; Essmann, U.; Stanley, H. E. Phase Behaviour of Metastable Water. *Nature* **1992**, *360*, 324.

(7) Debenedetti, P. G. Supercooled and Glassy Water. *J. Phys.: Condens. Matter* **2003**, *15*, R1669.

(8) Brovchenko, I.; Oleinikova, A. Multiple Phases of Liquid Water. *ChemPhysChem* **2008**, *9*, 2660−2675.

(9) Saika-Voivod, I.; Sciortino, F.; Poole, P. H. Computer Simulations of Liquid Silica: Equation of State and Liquid\Liquid Phase Transition. *Phys. Rev. E: Stat. Phys., Plasmas, Fluids, Relat. Interdiscip. Top.* **2000**, *63*, 011202.

(10) Sastry, S.; Austen Angell, C. Liquid-Liquid Phase Transition in Supercooled Silicon. *Nat. Mater.* **2003**, *2*, 739.

(11) Jakse, N.; Pasturel, A. Liquid-Liquid Phase Transformation in Silicon: Evidence from First-Principles Molecular Dynamics Simulations. *Phys. Rev. Lett.* **2007**, *99*, 205702.

(12) Ganesh, P.; Widom, M. Liquid-Liquid Transition in Supercooled Silicon Determined by First-Principles Simulation. *Phys. Rev. Lett.* **2009**, *102*, 075701.

(13) Vasisht, V. V.; Saw, S.; Sastry, S. Liquid-Liquid Critical Point in Supercooled Silicon. *Nat. Phys.* **2011**, *7*, 549.

(14) Umnov, A. G.; Brazhkin, V. V.; Popova, S. V.; Voloshin, R. N. Pressure-Temperature Diagram of Liquid Bismuth. *J. Phys.: Condens. Matter* **1992**, *4*, 1427.

(15) Umnov, A. G.; Brazhkin, V. V. Pressure-Temperature Diagram of Liquid Antimony. *High Pressure Res.* **1995**, *13*, 233.

(16) Brazhkin, V. V.; Popova, S. V.; Voloshin, R. N. Pressure-Temperature Phase Diagram of Molten Elements: Selenium, Sulfur and Iodine. *Phys. B (Amsterdam, Neth.)* **1999**, *265*, 64−71.

(17) Katayama, Y.; Mizutani, T.; Utsumi, W.; Shimomura, O.; Yamakata, M.; Funakoshi, K. A First-Order Liquid-Liquid Phase Transition in Phosphorus. *Nature* **2000**, *403*, 170.

DOI: 10.1021/acs.jpclett.8b01094
J. Phys. Chem. Lett. 2018, 9, 2909−2913

(18) Tsuji, K.; Hattori, T.; Mori, T.; Kinoshita, T.; Narushima, T.; Funamori, N. Pressure Dependence of the Structure of Liquid Group-14 Elements. *J. Phys.: Condens. Matter* **2004**, *16*, S989.
(19) Falconi, S.; Lundegaard, L. F.; Hejny, C.; McMahon, M. I. X-Ray Diffraction Study of Liquid Cs up to 9.8 GPa. *Phys. Rev. Lett.* **2005**, *94*, 125507.
(20) Di Cicco, A.; Trapananti, A.; Principi, E.; De Panfilis, S.; Filipponi, A. Polymorphism and Metastable Phenomena in Liquid Tin Under Pressure. *Appl. Phys. Lett.* **2006**, *89*, 221912.
(21) Okada, J. T.; et al. Persistence of Covalent Bonding in Liquid Silicon Probed by Inelastic X-Ray Scattering. *Phys. Rev. Lett.* **2012**, *108*, 067402.
(22) Cadien, A.; Hu, Q. Y.; Meng, Y.; Cheng, Y. Q.; Chen, M. W.; Shu, J. F.; Mao, H. K.; Sheng, H. W. First-Order Liquid-Liquid Phase Transition in Cerium. *Phys. Rev. Lett.* **2013**, *110*, 125503.
(23) Li, R.; Li, L.; Yu, T.; Wang, L.; Chen, J.; Wang, Y.; Cai, Z.; Chen, J.; Rivers, M. L.; Liu, H. Study of Liquid Gallium as a Function of Pressure and Temperature Using Synchrotron X-Ray Micro-tomography and X-Ray Diffraction. *Appl. Phys. Lett.* **2014**, *105*, 041906.
(24) Emuna, M.; Matityahu, S.; Yahel, E.; Makov, G.; Greenberg, Y. A Reversible Transition in Liquid Bi Under Pressure. *J. Chem. Phys.* **2018**, *148*, 034505.
(25) Aasland, S.; McMillan, P. F. Density-Driven Liquid-Liquid Phase Separation in the System Al_2O_3-Y_2O_3. *Nature* **1994**, *369*, 633−636.
(26) Rapoport, E. Model for Melting-Curve Maxima at High Pressure. *J. Chem. Phys.* **1967**, *46*, 2891−2895.
(27) Falconi, S.; Ackland, G. J. Ab Initio Simulations in Liquid Caesium at High Pressure and Temperature. *Phys. Rev. B: Condens. Matter Mater. Phys.* **2006**, *73*, 184204.
(28) Bryk, T.; De Panfilis, S.; Gorelli, F. A.; Gregoryanz, E.; Krisch, M.; Ruocco, G.; Santoro, M.; Scopigno, T.; Seitsonen, A. P. Dynamical Crossover at the Liquid-Liquid Transformation of a Compressed Molten Alkali Metal. *Phys. Rev. Lett.* **2013**, *111*, 077801.
(29) Ma, Y.; Eremets, M.; Oganov, A. R.; Xie, Y.; Trojan, I.; Medvedev, S.; Lyakhov, A. O.; Valle, M.; Prakapenka, V. Transparent Dense Sodium. *Nature* **2009**, *458*, 182.
(30) Matsuoka, T.; Shimizu, K. Direct Observation of a Pressure-Induced Metal-to-Semiconductor Transition in Lithium. *Nature* **2009**, *458*, 186.
(31) Ackland, G. J.; Macleod, I. R. Origin of the Complex Crystal Structures of Elements at Intermediate Pressure. *New J. Phys.* **2004**, *6*, 138.
(32) Boehler, R.; Zha, C.-S. Systematics in the Melting Behavior of the Alkali Metals from DAC Measurements. *Physica B+C (Amsterdam)* **1986**, *139−140*, 233−236.
(33) Tsujia, K.; Katayama, Y.; Morimoto, Y.; Shimomura, O. Structure of Liquid Rubidium under High Pressure. *J. Non-Cryst. Solids* **1996**, *205−207*, 295−298.
(34) Schwarz, U.; Grzechnik, A.; Syassen, K.; Loa, I.; Hanfland, M. Rubidium-IV: A High Pressure Phase with Complex Crystal Structure. *Phys. Rev. Lett.* **1999**, *83*, 4085−4088.
(35) DePanfilis, S.; Gorelli, F.; Santoro, M.; Ulivi, L.; Gregoryanz, E.; Irifune, T.; Shinmei, T.; Kantor, I.; Mathon, O.; Pascarelli, S. Local Structure of Solid Rb at Megabar Pressures. *J. Chem. Phys.* **2015**, *142*, 214503.
(36) Nelmes, R. J.; McMahon, M. I.; Loveday, J. S.; Rekhi, S. Structure of Rb-III: Novel Modulated Stacking Structures in Alkali Metals. *Phys. Rev. Lett.* **2002**, *88*, 155503.
(37) McMahon, M. I.; Rekhi, S.; Nelmes, R. J. Pressure Dependent Incommensuration in Rb-IV. *Phys. Rev. Lett.* **2001**, *87*, 055501.
(38) McMahon, M. I.; Nelmes, R. J. Chain "Melting" in the Composite Rb-IV Structure. *Phys. Rev. Lett.* **2004**, *93*, 055501.
(39) Soper, A. K.; Ricci, M. A. Structures of High-Density and Low-Density Water. *Phys. Rev. Lett.* **2000**, *84*, 2881−2884.
(40) Eggert, J. H.; Weck, G.; Loubeyre, P.; Mezouar, M. Quantitative Structure Factor and Density Measurements of High-Pressure Fluids in Diamond Anvil Cells by X-Ray Diffraction: Argon and Water. *Phys. Rev. B: Condens. Matter Mater. Phys.* **2002**, *65*, 174105.
(41) Soper, A. K.; Barney, E. R. Extracting the Pair Distribution Function from White-Beam X-Ray Total Scattering Data. *J. Appl. Crystallogr.* **2011**, *44*, 714−726.
(42) Soper, A. K.; Barney, E. R. On the Use of Modification Functions when Fourier Transforming Total Scattering Data. *J. Appl. Crystallogr.* **2012**, *45*, 1314−1317.
(43) Chihara, J.; Kahl, G. Structure Factor and Electronic Structure of Compressed Liquid Rubidium. *Phys. Rev. B: Condens. Matter Mater. Phys.* **1998**, *58*, 5314−5321.
(44) Chen, M.; Ko, H.-Y.; Remsing, R. C.; Calegari Andrade, M. F.; Santra, B.; Sun, Z.; Selloni, A.; Car, R.; Klein, M. L.; Perdew, J. P.; Wu, X. Ab Initio Theory and Modeling of Water. *Proc. Natl. Acad. Sci. U. S. A.* **2017**, *114*, 10846−10851.
(45) Bryk, T.; Demchuk, T.; Jakse, N.; Wax, J.-F. A Search for Two Types of Transverse Excitations in Liquid Polyvalent Metals at Ambient Pressure: An Ab Initio Molecular Dynamics Study of Collective Excitations in Liquid Al, Tl, and Ni. *Front. Phys.* **2018**, *6*, 6.
(46) Hosokawa, S.; Pilgrim, W.-C.; Hensel, F.; Hazemann, J.-L.; Raoux, D.; Mezouar, M.; Le Bihan, T.; Häusermann, D. X-ray Diffraction Measurements on Expanded Fluid Rb. *J. Non-Cryst. Solids* **1999**, *250−252*, 159−162.
(47) Zha, C.-S.; Bassett, W. A.; Shim, S.-H. Rhenium, an in Situ Pressure Calibrant for Internally Heated Diamond Anvil Cells. *Rev. Sci. Instrum.* **2004**, *75*, 2409−2418.
(48) http://www.esrf.eu/UsersAndScience/Experiments/MEx/ID27 (accessed May 8, 2018).
(49) https://github.com/Dioptas/Dioptas (accessed May 8, 2018).

DOI: 10.1021/acs.jpclett.8b01094
J. Phys. Chem. Lett. 2018, 9, 2909−2913